NÖHÜ Müh. Bilim. Derg. / NOHU J. Eng. Sci., 2021; 10(2), 527-534

MÜHENDİSLİK FAKÜLTESİ

Niğde Ömer Halisdemir Üniversitesi Mühendislik Bilimleri Dergisi
Niğde Ömer Halisdemir University Journal of Engineering Sciences

Araştırma makalesi / Research article

www.dergipark.org.tr/tr/pub/ngumuh / www.dergipark.org.tr/en/pub/ngumuh

Indirect field oriented control and direct torque control comparison with/without artificial neural networks on asynchronous motors

Asenkron motorlarda yapay nöral ağlar ile/olmadan dolaylı alan yönlendirmeli kontrol ve doğrudan tork kontrolünün karşılaştırması

Yavuz Üser[1,*], Haydar Can Acar[2]

[1,2] *Akdeniz Üniversitesi, Elektrik-Elektronik Mühendisliği Bölümü, 07070, Antalya, Türkiye*

Abstract

The flux, speed, and torque control performance of asynchronous motors are affected by parameter deviations and nonlinear variations of the asynchronous motor. In this study, Direct Torque Control (DTC) and Indirect Field Oriented Control (IFOC) structures are examined and asynchronous motor parameter deviations in both control structures are varied to desensitize with Artificial Neural Networks (ANN). In the literature, PI controllers are used in the IFOC structure. ANN is proposed for parameter desensitization, to the best of our knowledge no comparison and assessment has been made in the literature for these two methods. Comparisons are usually on the Direct Field Oriented Control (DFOC). This study proposes the parameter desensitization of IFOC and DTC with / without artificial neural networks and examines the effect on output performance. With the proposed control structure, it has been observed that the values of flux, torque and speed of asynchronous motor outputs capture the reference value at the desired performance and decrease the error values. With the proposed desensitization with ANN, IFOC performed over 50% better particularly in the time of overshoot and sitting than DTC. The proposed algorithms are implemented with Matlab / Simulink and the same reference values are used for each method.

Keywords: Asynchronous motor, Direct torque control, Indirect field oriented control, Speed control, Torque control, Matlab/Simulink

Özet

Asenkron motorların akı, hız ve tork kontrolü performansı, motorun parametre sapmalarından ve doğrusal olmayan varyasyonlarından etkilenmektedir. Bu çalışmada, Doğrudan Moment Kontrolü (DMK) ve Dolaylı Alan Yönlendirmeli Kontrol (DAYK) yapıları incelenmiş ve her iki kontrol yapısındaki motor parametre sapmalarını yapay nöral ağlar (YNA) ile duyarsızlaştırılmaya çalışılmıştır. Literatürde Dolaylı Alan Yönlendirmeli Kontrol yapısında PI denetleyiciler kullanılmaktadır. Parametre duyarsızlaştırması için ANN önerilmesi ve bu iki yöntem için literatürde karşılaştırma ve değerlendirme yapılmamıştır. Karşılaştırmalar genellikle Doğrudan Alan Yönlendirmeli Kontrol üzerinedir. Bu çalışma, yapay nöral ağları olan/olmayan DAYK ve DMK' nın parametre duyarsızlaştırması önererek ve çıkış performanslarına etkisini incelemektedir. Önerilen kontrol yapısı ile asenkron motor çıkışındaki akı, tork ve hızın istenen performansta verilen referans değeri yakaladığı ve hata değerlerinin azaldığı görülmektedir. YNA ile yapılan duyarsızlaştırma ile DAYK 'ın DMK' e göre, özellikle aşma ve oturma zamanında %50 'nin üzerinde daha iyi performans gösterdiği saptanmıştır. Önerilen algoritmalar Matlab/Simulink ile gerçeklenmiş ve her metot için aynı referans değerleri kullanılmıştır.

Anahtar kelimeler: Asenkron motor, Doğrudan moment kontrolü, Dolaylı alan yönlendirmeli kontrol, Hız kontrolü, Tork kontrolü, Matlab/Simulink

1 Introduction

Asynchronous motors are the electrical drive systems preferred by the industry due to their superior features such as simple structures, low maintenance, cheap prices, robust structures, high power/weight ratio and ability to operate in all kinds of environmental conditions. Nowadays, asynchronous motors are used in elevators, textile looms, eccentric presses, CNC looms, electric or hybrid cars. In addition, unlike DC motors, asynchronous motors can be used for many years as there is no brush structure [1] Asynchronous motors are the machines that convert electrical energy perfectly into mechanical energy besides the advantages mentioned above. However, mechanical energy is often required at different speeds and moments. The way to do this in a three-phase motor is to apply variable frequency and voltage [2].

In the asynchronous motor, speed control is done by changing the stator voltage, stator winding pole pair, stator frequency and rotor resistance. Speed control can be done by changing the amplitude and frequency of the stator voltage. In order to change the motor speed, it is desired to keep the amplitude constant while decreasing the frequency of the voltage applied to the motor. This causes the motor to draw too much current from the source. In many applications, it is sufficient to keep the voltage frequency ratio constant. However, in the high performance applications where speed and torque change suddenly, it can be difficult to keep this ratio constant [3]. Vector control methods can be developed

*Sorumlu yazar / Corresponding author, e-posta / e-mail: yuser@akdeniz.edu.tr (Y. Üser)
Geliş / Recieved: 07.11.2019 Kabul / Accepted: 18.01.2021 Yayımlanma / Published: 27.07.2021
doi:10.28948/ngmuh.643868

which can be adjusted flux and torque as desired. Thus, nonlinear values in the variables of the asynchronous motor can be better observed and controlled. In the vector control methods, the rotor flux spatial position is calculated and controlled by the driver by comparing the rotor angular velocity obtained by speed feedback and the stator current vector. The major disadvantage of vector control is the requirement to use a tachogenerator or encoder to achieve high accuracy. This makes it difficult to implement the driver system and increases its price. Vector control is divided into two categories which are known as direct vector control and indirect vector control. Linear controllers are used in the direct vector control. In the indirect vector control, calculations are performed with reactive energy equations [4].

The vector control method and the asynchronous motor's movement and moment are eliminated by the interlocking between each other. The moment correlation of the asynchronous motor with the lifting of the interlock between the flux and the moment becomes similar to the moment correlation of a DC motor. Thus, with the vector control of the asynchronous motor, the moment component of the stator current can be controlled linearly by keeping the flux component constant, as in the DC motors. Here, it is necessary to know the amplitude or position of one of the rotors, stator or air gap flux vectors in order to remove the interlock between the flux and the moment. Depending on the manner in which these vectors are obtained, the vector control is performed in two different ways, directly and indirectly. In the direct vector control method, the flux vector information generated in the motor is directly measured by the sensors. In the indirect vector control method, the position of the flux vector is found from the measured rotor speed/position and the calculated angular shift velocity. In the direct vector control method, flux information is obtained by measurement by the motor, therefore it requires special motors [5].

Consequently, direct vector applications are restricted and the indirect vector control is particularly preferred in practice. The major disadvantage of the indirect vector control is the need for a speed sensor with a high speed accuracy. The necessity of speed sensor sensitivity for detecting motor variables could create major disadvantages [6].

In the indirect vector control of asynchronous motors, the nonlinear structure of these motors and the time-varying parameters during the study are important problems encountered in the direct/indirect vector control method which is very sensitive to the parameter change. In these control methods, since the slip frequency depends on the rotor time constant, the change in the rotor time constant may result in incorrect calculation of the slip and as a result, the misalignment of the field. In addition, due to the non-linearity of the speed-moment characteristic of the asynchronous motors, sudden speed-moment changes can lead to instability of the motor. In order to overcome such drawbacks, the speed controller used in the control structure is required to be resistant to parameter changes and disturbing inputs [7, 8].

The research in recent years has shifted towards a more durable and non-linear controller design because it is quite difficult to address these problems with a conventional hysteresis and PI controller. For this purpose, due to non-linear structures of artificial neural networks (ANNs), fuzzy controllers (FC) and neural fuzzy controllers (NFC), adaptation and learning abilities, as well as the control of electric motors and the control of electric motors due to the lack of complex mathematical operations during the design phase, these methods have become widely studied and used [9]. NFC is mainly based on the realization of the functions of FC by ANN. Since it has a structure in which FC and ANN have superior characteristics, it has the capability of adaptation, learning and inference. The problems encountered in the vector control of asynchronous motors could be solved by these features and the non-linear structure of NFC. In the literature, NFC was used as the speed and speed monitor, parameter identifier and speed controller in the vector control of asynchronous motors. Although it is a controller which is resistant to parameter changes in its use as a speed controller, it cannot be able to resolve the steady state errors as it is still a problem to be solved for NFC similar to ANN and UN [10,11].

In this study, the speed control of an asynchronous motor was performed with both of these structures. Artificial neural networks were used because of the slowness of PI controllers and control structures' resistance to parameter changes. Thus, it is intended to obtain a non-linear controller that is resistant to load change, which does not require the mathematical equation of the motor for the controller design. In addition, an integral controller has been installed at the ANN output to eliminate any continuous faults. With the proposed audit structure, the training of the ANN was carried out in real time with the reference input signal using the feed forward propagation algorithm. By using the ANN parameters obtained as a result of the training, the simulation results were presented by evaluating the durability of this controller against constant and nonlinear loads were applied to the engine at different speed and torque values.

2 Materials and methods

2.1 *Control structures*

In this study, the block diagram of the asynchronous motor in the speed control is used. As a speed controller in the block diagram, PI controllers are preferred mostly because of their simple structure. However, PI parameters designed according to constant motor parameters can be insufficient under the motor dynamics and non-linear load conditions. This problem can be addressed by having the controller with adaptive parameters. For this purpose, NFC is used because of its non-linear structure, its ability to make learning, adaptation and inference, and its non-linear control system. As a controller, despite all these significant advantages, NFC as a supervisor is not sufficient to remedy the steady-state errors in the speed controls of drive systems, as in the ANN and the UN. This problem is solved by connecting the integral controller to the output of the NFC [12, 13]. Thus, a temporary and continuous state of changing the load and the parameters of the control structure is intended to be resistant. In the DTC method, the motor's flux and torque were calculated with the help of measurable magnitudes by motor parameters. The control method is based on applying a switching series, which shall directly eliminate errors that may occur in the torque, through the reference given as value and the calculated flux, to the power switching elements in the inverter, and the torque reference is obtained from PI controller output [14]. The application of direct torque control of an asynchronous motor is given in Figure 1.

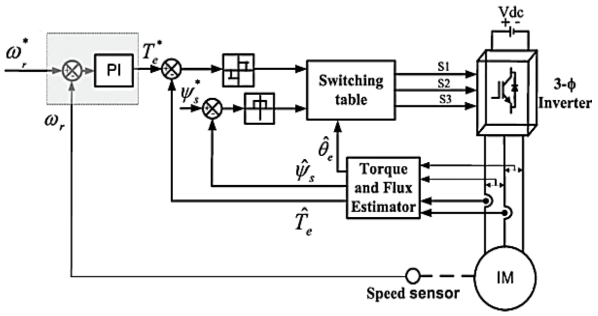

Figure 1. Direct torque control structure of an asynchronous motor

Vector control technique is based on the simulation of the torque and flux control components of the motor by simulating the DC motor model of AC motor. In this way, the torque and speed of the AC motor will be directly related to the electromagnetic state of the motor and can be easily controlled as a DC motor [15].

To achieve DC motor performance, Clarke and Park transformations must be applied. The Clarke transform represents the transition from the three-phase ABC reference to the two-phase αβ reference, while the Park transformation represents the transition from the two-phase αβ reference to the rotary d-q reference [16, 17].

The voltage equations in the d-q coordinates of the asynchronous motor are given as follows:

$$u_{ds} = R_s i_{ds} + p\lambda_{ds} - \omega_e \lambda_{qs} \tag{1}$$

$$u_{qs} = R_s i_{qs} + p\lambda_{qs} - \omega_e \lambda_{ds} \tag{2}$$

$$0 = R_r i_{dr} + p\lambda_{dr} - (\omega_e - \omega_r)\lambda_{qr} \tag{3}$$

$$0 = R_r i_{qr} + p\lambda_{qr} - (\omega_e - \omega_r)\lambda_{dr} \tag{4}$$

$$R_r i_{dr} + p\lambda_r = 0 \tag{5}$$

$$R_r i_{qr} + \omega_{sl}\lambda_r = 0 \tag{6}$$

$$i_{ds} = i_f = [1 + \tau_r p]\frac{\lambda_r}{L_m} \tag{7}$$

$$i_{qs} = i_T = \frac{\tau_r \lambda_r \omega_{sl}}{L_m} \tag{8}$$

$$T_e = n_p \frac{L_m}{L_r}\lambda_{dr} i_{qs} = n_p \frac{L_m}{L_r}\lambda_{dr} i_T \tag{9}$$

As shown in Equation 9, the electromagnetic torque is proportional to the rotor flux and the stator current in the q axis. This statement is similar to the torque statement of the DC motor. The DC motor is directly proportional to the field flux and inductive current in torque. Hasse flux estimation on this control structure has suggested that the sensor is not needed, it can be measured by estimating the rotor flux or it can be measured mathematically or by motor parameters [18, 19]. In this way, the cost of the control structure is reduced and the ease of application is ensured. The application of the indirect field-oriented control structure to the asynchronous motor is shown in Figure 2. ASR and ATR blocks are PI controllers that control speed and torque changes [20]. The torque command is derived from the function Te^* speed error signal, and the current command i_T^* is derived from the function of the torque error signal.

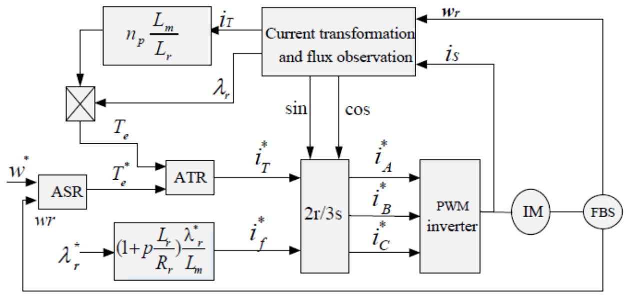

Figure 2. Indirect field oriented control structure

2.1.1 Design PI Controller with Conventional Approach

The simplest dynamic speed and torque model that can be used in an asynchronous motor is as in the block diagrams shown in Figure 3-4 [21].

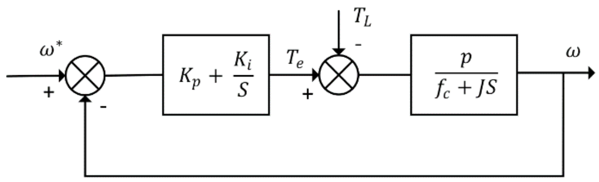

Figure 3. Block diagram of speed controller

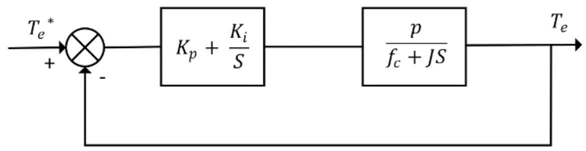

Figure 4: Block diagram of torque controller

If TL = 0, the closed loop transfer function for both block diagrams is as follows as,

$$G(s) = \frac{(K_p s + K_i)\frac{P}{J}}{s^2 + \frac{f_c + K_p}{L_r} s + \frac{K_i}{J}} \tag{10}$$

$$G(s) = \frac{(K_p s + K_i)\frac{P}{J}}{s^2 + \frac{f_c + K_p}{L_r} s + \frac{K_i}{J}} \tag{11}$$

The characteristic equivalence of the transfer function is as follows,

$$P(s) = s^2 + \frac{f_c + K_p P}{J} s + \frac{K_i P}{J} = 0 \tag{12}$$

By applying of the two-poles complex root $s_{1,2} = \rho(-1 \pm j)$, Ki and Kp coefficient expressions are obtained. P is a positive constant

$$K_p = \frac{2pJ - f_c}{P} \qquad K_i = \frac{2j\rho^2}{P} \tag{13}$$

P is a positive constant, PI coefficients are given below in Table 1.

Table 1. PI controller coefficients

Coefficients	K_p	K_i
In DTC	0.711	17.121
In ASR	0.210	20.010
In ATR	1.010	10.024

2.1.2 Neural Network Structure

There are many network structures in the use of neural networks in the audit area. However, due to the simplicity of its structure and its effectiveness in the control of non-linear systems, the so-called adaptive neural network system (ANNS) is preferred [22]. In this study, this network structure is used as a speed controller and its structure is presented in Figure 3. This network structure, which is used as a speed controller, has been selected as one, two and three inputs and single outputs according to the control block shown in Figure 5 and 7. ANN consists of a total of five layers and the functions performed in these layers are described below.

1-*Layer:* The first layer is the membership function layer and the membership function degree for each input variable is calculated in this layer. In this case, three functions for each input are selected, one for bell function and two for sigmodal function.

The first layer output of the ANN is y1, and the membership function parameters are a, b and c. The membership function degrees that connect to the output are calculated as follows:

$$y_{ij}^1 = \frac{1}{1 + e^{-a_{ij}(x_i^1 - c_{ij})}}, i = 1,2 \; and \; j = 1,3 \tag{14}$$

$$y_{i2}^1 = \frac{1}{1 + \left|\frac{x_i^1 - c_{i2}}{a_{i2}}\right|^{2b_{i2}}} \tag{15}$$

The parameters a, b and c are also referred to as input parameters of the ANN.

2- *Layer:* The second layer of the ANN constitutes the rule base and fuzzy rules are determined in this layer. The second layer output is y2, any k. The node is calculated as follows:

$$y_k^2 = \prod_i y_{ij}^1 \;\; k = 1,2,\ldots,9 \tag{16}$$

3- *Layer:* This layer is called the normalization layer and it calculates the degree of accuracy of fuzzy rules. Any k. normalization process for the node, k. fuzzy rule is obtained by dividing the degree of precision by the sum of the rules of certainty.

$$y_k^3 = \frac{y_k^2}{\sum_k y_k^2} \tag{17}$$

4-*Layer:* The fourth layer of the NFC is called the size of the firing degree of a rule. The degree of firing of the normalized rules in this layer is multiplied by a linear function f and the fuzzy rules are cleared.

$$y_k^4 = y_k^4 f_k \tag{18}$$

$$f_k = p_k x_1 + q_k x_2 + r_k \tag{19}$$

Here, p, q and r are the parameters of the function f and are called the output parameters of the NFC.

5-*Layer:* This layer is the output node of the SB and it transfers its sum to its output.

$$y^5 = \sum_k y_k^4 \tag{20}$$

Artificial neural network block which is established in Figure 5 is implemented to the control structures and simulated using Matlab/Simulink software. Differences from previously designed control structures were observed and advantages and disadvantages of artificial neural networks are studied.

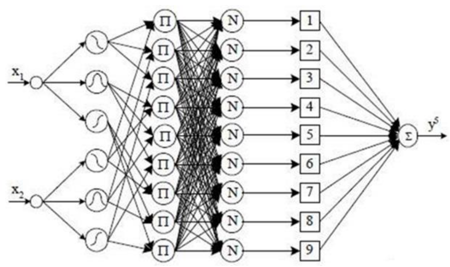

Figure 5. The structure of artificial neural networks and layers

3 Results and discussion

The ANN structure is added to the indirect field-oriented control system and simulated with the same reference speed and torque values. Figure 6 and 7 present the system with artificial neural network and without artificial neural network.

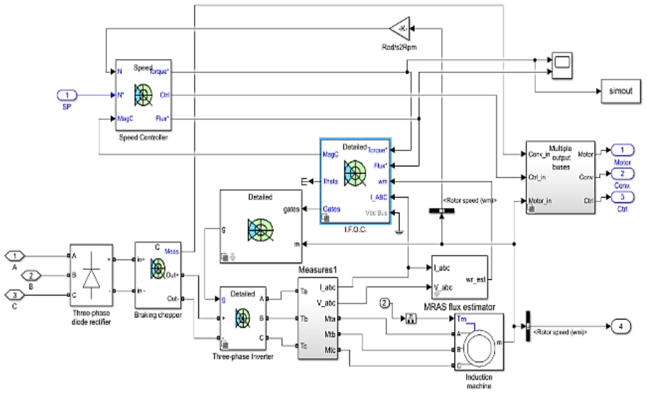

Figure 6. Indirect field oriented control without artificial neural network structure

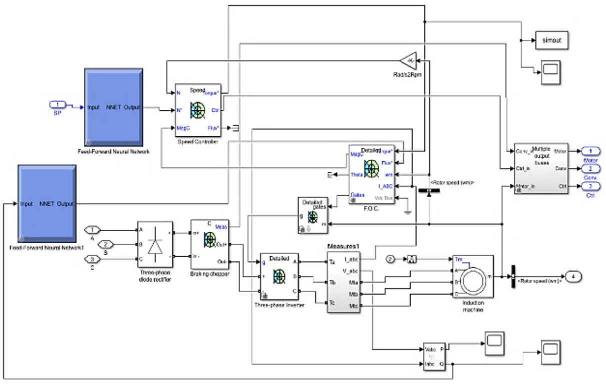

Figure 7. Indirect field oriented control with artificial neural network structure

Same additions also realized for the direct torque control structure. Artificial neural network is connected instead of PID and hysteresis controllers. To be able to observe the performance results, same reference speed and torque values are given to the system. Figures 8 and 9 show the direct torque control structures with and without artificial neural networks. The sampling period is Ts = 2e-6 in the methods.

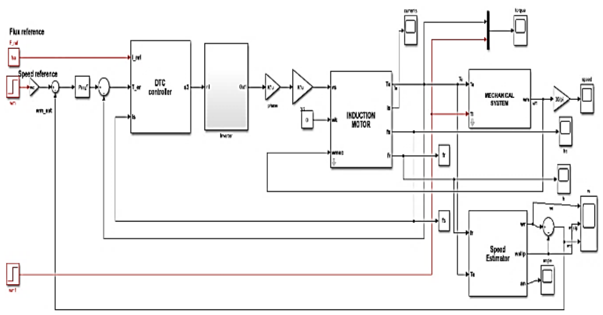

Figure 8. Direct torque control without artificial neural network structure

After the modelling of these structures, speed responses, torque responses and flux estimations of the systems were simulated. Figure 10 and 11 show the flux estimations of the systems, respectively. Estimation of rotor flux which is one of the important design parameters will reduce the negative effects of long control processes and costly drive operations on engineering applications. Flux estimation errors of the methods were calculated according to the actual flux and estimated flux.

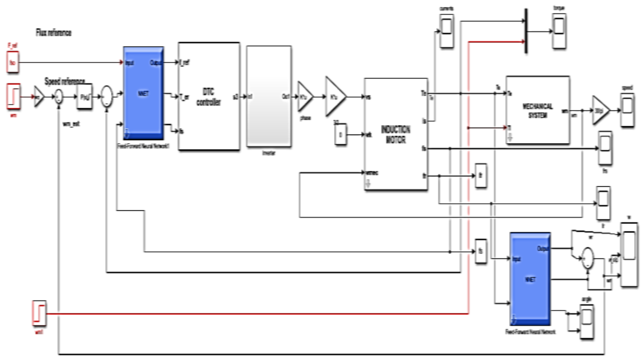

Figure 9. Direct torque control with artificial neural network structure

The flux estimation errors for ANN-IFOC, ANN-DTC, IFOC, DTC structures are calculated as 2%, 3%, 6% and 8%, respectively.

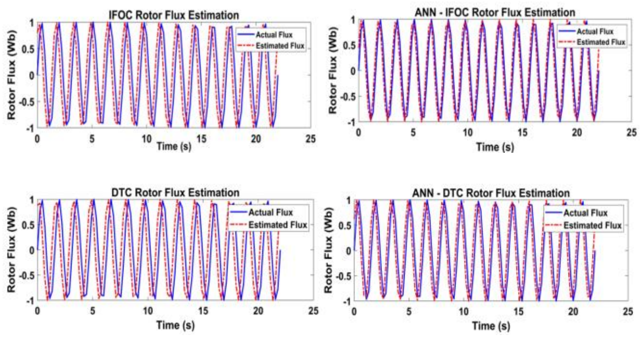

Figure 10. Flux estimations of the systems

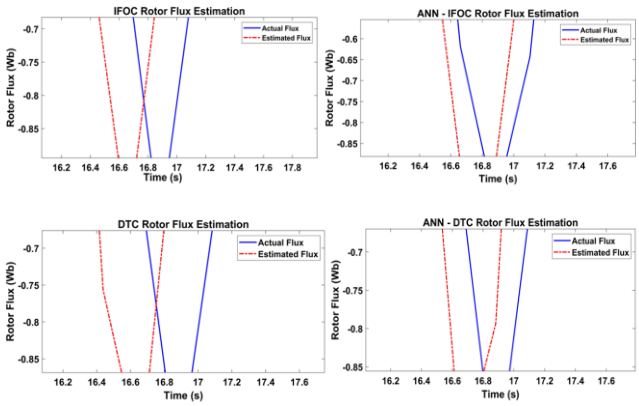

Figure 11. Flux estimations with estimation errors

As seen in Figure 10 and 11, flux estimations of the systems show very close results to each other. The main differences are control structures and the addition of artificial neural network algorithm. The second comparison parameter is speed responses of the systems. Figure 12 shows the speed response of four systems. The reference speed is set 500 rad/sec and systems are compared according to this value.

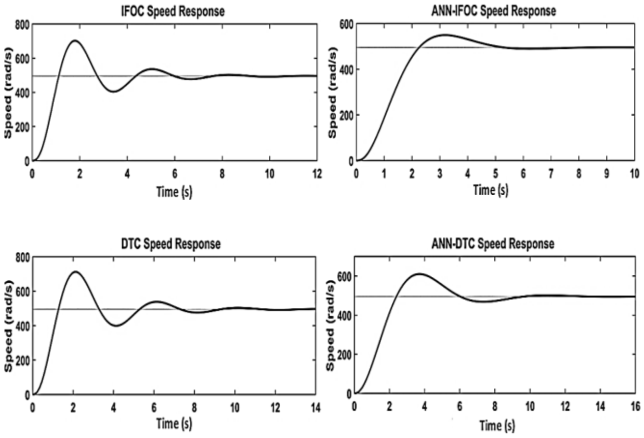

Figure 12. Speed responses of the systems

Table 2 expresses Figure 12 mathematically. Overshoot, rise time, settling time and final values of the systems are shown as a comparison parameter.

Table 2. Comparison of speed responses

Methods	Overshoot	Rise Time	Settling Time	Steady State Error
Indirect Field Oriented Control with ANN	*10.9%*	*1.45 sec*	*4.81 sec*	*0.002% error*
Direct Torque Control with ANN	*23.2%*	*1.58 sec*	*8.88 sec*	*0.004% error*
Indirect Field Oriented Control	*41.7%*	*1.68 sec*	*9.71 sec*	*0.008% error*
Direct Torque Control	43.6%	1.80 sec	12.85 sec	*0.01% error*

As presented in Table 2, IFOC shows slightly better results similar to studies previously mentioned in the literature (Bose et al.,1997). When artificial neural networks are added to the system, difference between these two systems was increased as observed. Artificial neural network structure gives better performance with both of these control methods. Overshoot values, rise time and settling time values are decreased and a better convergence is made thanks to artificial neural networks. With the addition of ANN to both methods, there is close to 100% improvement by decreasing the overshoot from 23.2% to 10.9% and settling time from 8.88 s to 4.81 s in the IFOC method speed graph. Same procedure is repeated for torque values. Figure 13 shows the torque responses of the systems. Initially the torque values were set 350 Nm and it instantly increased up to 1000 Nm in the first second. Table 3 expresses the Figure 13 mathematically. Overshoot, rise time, settling time and final values of the systems are shown in Table 3 as a comparison parameter.

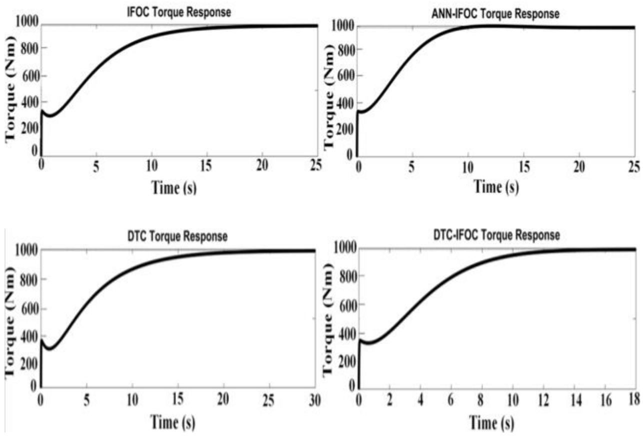

Figure 13. Torque responses of the systems

With the addition of ANN to both methods, the IFOC method decreased overshoot from 2.84% to 1.26% and the steady state error rate was the lowest with 0.001%.

Table 3. Comparison of torque responses

Methods	Overshoot	Rise Time	Settling Time	Steady State Error
Indirect Field Oriented Control with ANN	*1.26%*	*6.5 sec*	*8.52 sec*	*0.001% error*
Direct Torque Control with ANN	*2.84%*	*7.85 sec*	*11.5 sec*	*0.003% error*
Indirect Field Oriented Control	*4.12%*	*9.38 sec*	*14.9 sec*	*0.006% error*
Direct Torque Control	6.48%	11.4 sec	18.9 sec	*0.008% error*

Different torque and speed values are simulated in Figure 14 and 15, respectively. Black line which is given as a reference signal represents a real time signal. This signal provides more realistic information about changes and responses. It is seen that methods including ANN follow the reference torque -53N, 12N, 55N, 35N, 50N better and IFOC with ANN gives the closest output to the reference. Addition of the ANN structure has improved the speed. Reference speed -50 rad/s, 10 rad/s, 50 rad/s values were followed by IFOC with ANN and DTC with ANN. Unfortunately, DTC and IFOC couldn't follow the speed reference correctly. An undesired small shift in the motor parameters changes the output by changing the flux angle and switching states. The ANN structure eliminates these changes. The DTC method uses only stator resistance value as a motor parameter and possible changes in resistance due to the motor temperature will have a direct effect on the DTC performance.

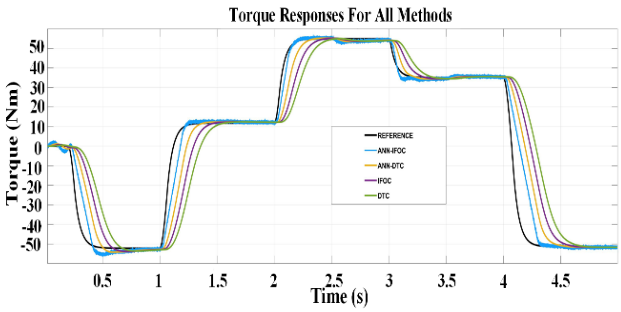

Figure 14. Torque settlings

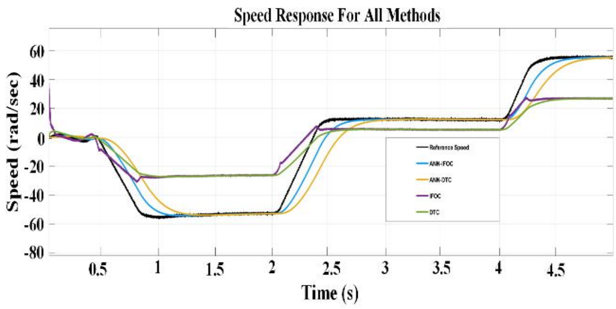

Figure 15. Speed settlings

ANN structure was added to minimize changes in the resistance for the DTC method and to keep rotor time constant in the IFOC method. In order to make a comparison of performances with DTC, IFOC and the proposed ANN-DTC, ANN-IFOC methods, different ranges of speed and load values were also applied to the IM. While DTC has a simple structure, the method is sensitive to the parameter changes. On the other hand, IFOC is robust to the varying parameters due to its structure. The dynamic performance of IFOC is preferred under this comparison. Both the overshoot and the settling time of IFOC are much smaller than DTC. ANN-IFOC and ANN-DTC structures show better results than IFOC and DTC structures. ANN-IFOC structure has the fastest response and it can catch the sharpest changes during the process.

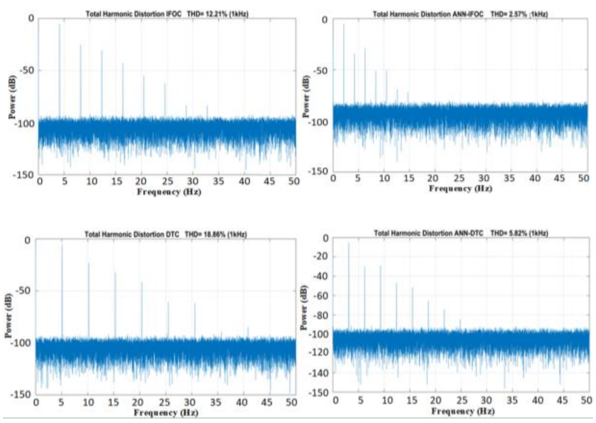

Figure 15. Total harmonic distortions of the methods

Figure 16 shows the total harmonic distortion values for each method. Since the drives are directly switched in the DTC method, it generates more harmonics than the IFOC method. Total harmonic values were 18.86% for DTC, 12.21% for IFOC, 5.82% for ANN-DTC and 2.57% for ANN-IFOC. The fundamental frequency is 1Khz and the switching frequency is 5kHz. As shown in Figure 16, the ANN-IFOC structure has produced the least harmonic.

4 Conclusion

In this study, the control of an asynchronous motor drive in the direct torque control structure and indirect field oriented control structure is realized using with and without artificial neural network structures. Using the ANN controller, there is no need for intensive mathematical operations required for controller design. Thus, the effect of the time-varying parameters encountered in the control of the asynchronous motor has a positive effect on the performance of the asynchronous motor. The response of the IFOC and DTC structures to the parameter sensitization by using artificial neural networks can be seen from Figures. Majority of studies in the literature compared direct torque control structure and field orientated control structure. In our study, the performance of the indirect field orientated control structure compared to the direct torque control structure have been evaluated and have shown clearly. Due to the fact that the IFOC structure is particularly successful, the flux estimation has been performed on the reactive power. As shown in Table 2 and 3, speed and torque responses provided better results with ANN structure. Particularly for the speed outcomes, the IFOC structure with ANN has reached the settling time value 46% faster than DTC. In addition, it has responded 26% faster for the torque outcomes. THD levels with ANN have suppressed harmonics above 20Khz in both methods. In this study, outcomes of all structures have been explored and compared and according to our analysis, the ANN-IFOC structure gave the best performance result among all structures. Hence, the ANN-IFOC structure has the potential to provide better quality drive in industrial applications regardless of the parameters.

Appendix

The asynchronous motor has following parameters;

P =4	Number of poles
f_0 =60	Base frequency (Hz)
V_s=470/1.73	Rated Voltage (V)
T=350-1000	Rated Torque (Nm)
R_s = 0.01485	Stator Resistance (ohm)
R_r=0.009295	Rotor resistance (ohm)
R_c=2000	Core loss equivalent resistance (ohm)
l_s=0.0003027	Stator Leakage Inductance (H)
$l_r = l_s$	Rotor Leakage (H)
L_m=0.01046	Constant Mutual Inductance (H)
$Prot$=40000	Rotational Losses (W)

Çıkar çatışması

Yazarlar çıkar çatışması olmadığını beyan etmektedir.

Benzerlik oranı (iThenticate): %17

References

[1] J. Barta, N. Uzhegov, P. Losak, C. Ondrusek, M. MacH, and J. Pyrhonen, Squirrel-Cage Rotor Design

and Manufacturing for High-Speed Applications, IEEE Trans. Ind. Electron. 66 6768–6778. 2019. https://doi.org/10.1109/TIE.2018.2879285.

[2] J. M. Pena, and E. V. Diaz, Implementation of V/f scalar control for speed regulation of a three-phase induction motor, in: Proc. 2016 IEEE ANDESCON, ANDESCON 2016, Institute of Electrical and Electronics Engineers Inc., 2017. https://doi.org/10.1109/ANDESCON.2016.7836196.

[3] A. Taheri, H. P. Ren, C. H. Song, Sensorless Direct Torque Control of the Six-Phase Induction Motor by Fast Reduced Order Extended Kalman Filter, Complexity. 2020. https://doi.org/ 10.1155 /2020/ 8 985417.

[4] A. Pal, S. Das, and A. K. Chattopadhyay, An improved rotor flux space vector based mras for field-oriented control of ınduction motor drives, IEEE Trans. Power Electron. 33 5131–41.2018 https:// doi.org /10.1109/ TPEL. 2017. 2657648.

[5] S. Peresasa, A. Tilli and A. Tonielli, Theoretical and experimental Comparison of indirect Field oriented Controllers for induction motors, IEEE Trans. on Power Electron., vol. 18, 151 163, 2003.

[6] Y. Liu, G. Tao, H. Wang, and F. Blaabjerg, Analysis of indirect rotor field oriented control-based induction machine performance under inaccurate field-oriented condition, in: Proc. IECON 2017 - 43rd Annu. Conf. IEEE Ind. Electron. Soc., Institute of Electrical and Electronics Engineers Inc., 1810–15. 2017 https://doi.org/10.1109/IECON. 2017 .8216306.

[7] L. Monjo, F. Córcoles, and J. Pedra, Parameter estimation of squirrel-cage motors with parasitic torques in the torque-slip curve, IET Electr. Power Appl. 9 377–87. 2015 https://doi.org/10.1049 /iet-epa.2014.0208.

[8] Yang, D. Ding, X. Li, Z. Xie, X. Zhang, and L. Chang, A Novel Online Parameter Estimation Method for Indirect Field Oriented Induction Motor Drives, IEEE Trans. Energy Convers. 32 1562–73. 2017 https://doi.org/10.1109/TEC.2017.2699681.

[9] A. Rubai, D. Ricketts, and D. Kanham, Development and implementation of an adaptive fuzzy-neural network controller for brushless drivers, IEEE Transaction on Industry Applications, 38, 441-447, 2002.

[10] B. Lazerini, L. M. Reyneri, and M. A. Chiaberge, A neuro- fuzzy Approach to hybrid intelligent control, IEEE Transactions on Industry Applications, 35, 413-425,1999.

[11] B. Kirankumar, Y. V. Siva Reddy, and M. Vijayakumar, Multilevel inverter with space vector modulation: Intelligence direct torque control of induction motor, IET Power Electron. 10 1129–37. 2017 https://doi.org/10.1049/iet-pel. 2016. 0287.

[12] K. H. Tan, Squirrel-Cage Induction Generator System Using Wavelet Petri Fuzzy Neural Network Control for Wind Power Applications, IEEE Trans. Power Electron. 31 5242–54. 2016 https://doi.org/10.1109/TPEL.2015.2480407.

[13] Y. Üser, K. Gülez, A new direct torque control algorithm for torque and flux ripple reduction, Internatıonal Revıew of Electrıcal Engıneerıng-IREE,.8, 644-653, 2013

[14] R. İnan, Asenkron motorun alan zayıflama bölgesinde kayan kip denetçi tabanlı hız-algılayıcısız doğrudan vektör kontrolü, Ömer Halisdemir Üniversitesi Mühendislik Bilim. Derg. 8 762–774. 2019 https://doi.org/10.28948 /ngu muh.515332.

[15] R. İnan, R. Demir ve M. Barut, Asenkron motorun karma kestirici tabanlı hız-algılayıcılı doğrudan vektör kontrolü, Ömer Halisdemir Üniversitesi Mühendislik Bilim. Derg. 7 612–623. 2018 https ://doi.org/10.28948/ngumuh.443233.

[16] E. Zerdali, Modele uyarlamalı sistem temelli model öngörülü moment kontrollü sürücü sisteminin tasarımı, Ömer Halisdemir Üniversitesi Mühendislik Bilim. Derg. 9 146–153.2020 https://doi.org/10.28948 /ngumuh.607378.

[17] Y. Üser, K. Gülez, and Ş. Özen, Sensorless flux region modification of Dtc controlled Im For torque ripple reduction, IU-JEEE, vol.14, pp.1753-60, 2014.

[18] C. Fahassa, Y. Sayouti, and M. Akherraz, Improvement of the induction motor drive's indirect field oriented control performance by substituting its speed and current controllers with fuzzy logic components, in: Proc. 2015 IEEE Int. Renew. Sustain. Energy Conf. IRSEC 2015, Institute of Electrical and Electronics Engineers Inc., 2016. https://doi.org/10.1109/IRSEC.2015.7454928

[19] L. Zhang, X. Zhu, Y. Fan, C. Li, Optimal flux-weakening control of a new five-phase FT-IPMmotor based on DTC and SVPWM for electric vehicle applications, IET Electr. Power Appl. 13 73–80. 2019 https://doi.org/10.1049/iet-epa.2018 . 5204.

[20] L. Saribulut, A. Teke, M. Tümay, Artificial neural network-based discrete-fuzzy logic controlled active power filter, IET Power Electron. 7 1536–46. 2014 https://doi.org/10.1049/iet-pel.2013 .0 522.

[21] M. Hamed Chebre, A. Meroufel, Y. Bendaha, Speed control of ınduction motor using genetic algorithm-based pı controller, Acta Polytechnica Hungarica, 2011, Vol. 8, No. 6, 141-153.

[22] P. Cao, X. Zhang, and S. Yang, A unified-model-based analysis of mras for online rotor time constant estimation in an ınduction motor drive, IEE Trans. Ind. Electron. 64 4361–71. 2017 https: //doi .org / 10.1109/TIE.2017.2668995.